The Calculation of Molecular Volumes and the Use of Volume Analysis in the Investigation of Structured Media and of Solid-State Organic Reactivity

A. Gavezzotti

Contribution from the Istituto di Chimica Fisica e Centro CNR, Università di Milano, 20133 Milano, Italy. *Received January 27, 1983*

Abstract: Starting from known molecular geometries and atomic radii, a fast and accurate method for calculating the volume of a molecule is proposed. The same procedure used to calculate this molecular volume is used to perform a volume analysis on various kinds of molecular systems and structured media. This analysis allows the location of empty and filled spaces and the precise evaluation of their volumes. The method is applied here to three different problems: (i) the calculation of cavity volume in cage compounds, and the study of their compatibility with complexed ions; (ii) the prediction of stoichiometry and stability of inclusion compounds in crystalline matrices; and (iii) the analysis of steric factors influencing the solid-state reactivity of organic compounds. Other applications in related fields are briefly examined.

Introduction

Accurate wave functions for molecules of medium to large size can nowadays be otained,[1] and detailed maps of molecular charge density can in principle give a pictorial view of molecular size and shape.[2] On the other hand, a very large body of X-ray diffraction data on the arrangement of molecules in crystals is at hand;[3] approximate theories of intermolecular interactions use such concepts as atomic radii and molecular shape, which, together with and on the same grounds as bond lengths and bond angles, are at the origin of all theories of crystal close packing.[4] To some extent, then, the study of structured media relies upon some very simple shorthands for electron density, by just considering its outermost envelope, or molecular volume. In fact, simple relationships exist[5] between this quantity and crystal cohesion energy when close-packing is observed in crystals. Of course, more refined experiments warn that the same atom may not always have the same shape in different crystal environments,[6] and more accurate calculations of crystal energies must include explicitly some terms which depend on the actual distribution of electrons in the molecule.[7] Still far from reach seems to be a first-principles quantum mechanical treatment of a system as complex as a crystal.[8]

In its second section, this paper presents a method for obtaining molecular volumes, based on standard molecular geometries and on standard atomic radii. This task has already been accomplished in an accurate compilation by Bondi,[9] in times (1964) when neither computational facilities nor structural data were abundant. Our method fully exploits both. Applications of the results, and of a generalization of the volume analysis method, to various fields of the physical chemistry of structured media will then be presented, with an emphasis on solid-state reactivity in organic crystals.[10] The interpretation of molecular volume in terms of electronic structure is postponed to future work, if not dismissed altogether. Consistently with its empirical derivation, the model will be judged heuristically on the basis of its performance.

Table I. Radii for Atomic Spheres (Å)

atom	used in present work (ref 13)	used in ref 9
H	1.17	1.00-1.20
C	1.75	1.70-1.77
N	1.55	1.60
O	1.40	1.50
F	1.30	1.40-1.47
Cl	1.77	1.73-1.77
Br[a]	1.95	1.84-1.92
I[a]	2.10	2.01-2.06

[a] See: Gavezzotti, A.; Simonetta, M. *Acta Crystallogr., Sect. A* 1975, *A31*, 645.

The Calculation of Molecular Volumes

A chemical entity (molecule or fragment) is described by a set of vectors, $\mathbf{S}_i$, connecting the atomic nuclei to a chosen origin, and a set of radii, R_i (one for each atomic species), each of which defines a sphere around nucleus i. The main source of molecular dimensions is spectroscopy or electron diffraction for the gaseous state,[11] and X-ray crystallography for the solid state.[12] The choice of R_i's generally involves a critical evaluation of X-ray data on intermolecular separations in crystals. There seems to be broad convergence of opinions as regards numerical values, and strong debate over physical or chemical interpretation. Our choice is shown in Table I: it reflects a pondered evaluation of large amounts of intermolecular data.[13]

Depending on geometry, the spheres defined by the R_i's may overlap, making volume calculations cumbersome. Thus, former approaches[4,9] based on the total volume of the spheres less the volume of intersecting caps require special caution with cyclic or crowded molecules; patent cases of such difficulties are those of cyclopropane and of a cage molecule such as decaborane.[14] A

(1) See for a general view: Richards, W. G.; Walker, T. E. H.; Farnell, L.; Scott, P. R. "Bibliography of ab initio Molecular Wave Functions: Supplement for 1970-1973"; Clarendon Press: Oxford, 1974.

(2) In such terms, defining molecular shape and size is equivalent to choosing a threshold value for the charge density to define molecular boundaries; see, for example: Bader, R. F. W.; Henneker, W. H.; Cade, P. E. *J. Chem. Phys.* **1967**, *46*, 3341.

(3) Kennard, O.; Watson, D. G.; Allen, F. H.; Weeds, S. M., Eds. "Molecular Structures and Dimensions"; International Union of Crystallography, Polycrystal Book Service: Pittsburgh, 1979; Vol. 1-10.

(4) Kitaigorodski, A. I. "Organic Chemical Crystallography"; Consultants Bureau: New York, 1961. Kitaigorodski, A. I. "Molecular Crystals and Molecules"; Academic Press: New York, 1973.

(5) Gavezzotti, A. *Nouv. J. Chim.* **1982**, *6*, 443.

(6) See, for instance, Coppens, P.; Stevens, E. D. In "Advances in Quantum Chemistry"; Lowdin, P.-O., Ed.; Academic Press: New York, 1977; Vol. 10, p 1.

(7) Such terms are broadly defined as electrostatic; see for a recent example: Berkovitch-Yellin, Z.; Leiserowitz, L. *J. Am. Chem. Soc.* **1982**, *104*, 4052.

(8) See, however: O'Shea, S. F.; Santry, D. P. *Theor. Chim. Acta* **1975**, *37*, 1.

(9) Bondi, A. *J. Phys. Chem.* **1964**, *68*, 441.

(10) Gavezzotti, A.; Simonetta, M. *Chem. Rev.* **1982**, *82*, 1.

(11) We have used a compendium of data from: Sutton, L. E., Ed. "Tables of Interatomic Distances and Configurations in Molecules and Ions"; The Chemical Society: London, 1965; Pople, J. A.; Gordon, M. *J. Am. Chem. Soc.* **1967**, *89*, 4253, Table I.

(12) For biphenyl and cyclohexane, the structural data from the X-ray analyses of Charbonneau and Kahn (Charbonneau, G. P.; Delugeard, Y. *Acta Crystallogr., Sect. B* **1976**, *B32*, 1420. Kahn, R.; Fourme, R.; André, D.; Renaud, M. *Ibid.* **1973**, *B29*, 131) respectively, have been used in the calculation of molecular volume.

(13) Mirsky, K. In "Computing in Crystallography, Proceedings of an International Summer School on Crystallographic Computing"; Delft University Press: Twente, 1978; p 169.

0002-7863/83/1505-5220$01.50/0

Table II. Molecular Volumes (Å^3)

molecule	V_m, present work	V_m', ref 9	$(V_m' - V_m)/V_m$, %
carbon dioxide	30.61		
water	16.82		
ammonia	21.91		
methane	28.01	28.42	+2
ethane	44.63	45.38	+2
propane	61.39	62.37	+2
ethylene	40.25	39.64	−2
propene	56.72	56.57	0
acetylene	36.15	38.35	+6
diacetylene	59.74	64.31	+8
benzene	85.39	80.28	−6
toluene	101.8	98.79	−3
biphenyl	157.1	152.2	−3
fluoroethane	47.45	49.17	+4
chloroethane	59.45	58.96	−1
bromobenzene	106.6	100.3	−6
iodobenzene	114.7	108.7	−5
cyclopropane	42.7 50.0[a]		
cyclohexane	99.1 99.2[a]	100.0	+1
acetone	62.86	64.81	+3
methanol	34.89	36.04	+3
acetic acid	51.18	55.10	+8

[a] As computed by the spheres-and-caps method (ref 4).

Table III. Group Increments for Molecular Volume Calculations (Å^3)

group	V_g, present work	V_g', ref 9	$(V_g' - V_g)/V_g$, %
$>CH_2$	16.76	16.98	+1
$-CH_3$	22.32	22.69	+2
$>CH$	11.52	11.25	−2
$=CH_2$	20.13	19.82	−2
$=CH$	14.27	14.06	−1
$\equiv CH$	18.07	19.17	+6
$\equiv C-$	11.80	12.98	+10
CH(aromatic)	14.23	13.38	−6
$>C=O$	18.22	19.42	+7
$-OH$	12.57	13.35	+6

straightforward approach, made possible by high-speed digital computing, consists of sampling an envelope space, containing all vectors $\mathbf{S}_i + \mathbf{R}_i$ for the chemical entity, with a very large number (N) of probe points, and counting the number (N_{occ}) of points inside at least one of the spheres.[15] If the volume of the envelope space is V_{env}, then the molecular volume, V_m, is given by

$$V_m = V_{env}\frac{N_{occ}}{N} \tag{1}$$

The finer the point mesh, the more accurate is V_m; a typical value is 1000 points/Å^3. For comparison, Table II collects V_m values as computed in different ways. It is customary to recast the results in the form of group increments, to allow an estimate of V_m for any molecular system or fragment. This is done (at least partially) in Table III.

One of the advantages of our method is that it applies also to the calculation of volumes of empty space. Thus for instance the volume of an interatomic cavity can be computed as

$$V_c = V_{env}\frac{N - N_{occ}}{N} \tag{2}$$

although this may require a skillful choice of boundaries of the envelope space. A somewhat more efficient strategy will be exposed in a further section.

(14) Beringhelli, T.; Filippini, G.; Gavezzotti, A.; Simonetta, M. *J. Mol. Struct.*, in press.

Table IV. Comparison of Molecular Volumes, V_m (as in Table II), with Collision Theory Volumes, $V_p = b/4$, Where b Is as in Equation 3 (Å^3)

compound	V_p[a]	V_p/V_m
methane	17.77	0.63
propane	35.07	0.57
ethylene	23.75	0.59
acetylene	21.33	0.59
benzene	47.93	0.56
toluene	60.76	0.60
biphenyl	103.0	0.66
chloroethane	35.93	0.60
chlorobenzene	60.34	0.61
iodobenzene	68.77	0.60
acetone	41.28	0.66
carbon dioxide	17.72	0.58
carbon monoxide	16.55	0.63
acetic acid	44.35	0.87
methyl alcohol	27.83	0.80
water	12.66	0.75

[a] All entries in this column from Weast: Weast, R. C., Ed. "Handbook of Chemistry and Physics"; CRC Press: Cleveland, 1974; p D157.

From the data in Table II, it can be seen that differences in V_m between our results and those in ref 9 never exceed 10%, in spite of the sometimes relevant differences in molecular geometries, atomic radii, and method of calculation. This is encouraging, since it means that the model can survive different choices of parameters.

Although a measure of V_m may be matched to many properties of gases, liquids, and solids, only one comparison with readily available data for gaseous molecules will be given here, namely, with covolume, the b parameter in the van der Waals equation

$$(P + a/V^2)(V - b) = RT \tag{3}$$

If b is taken as $4V_p$, where V_p is the proper volume of one molecule in collision theory, then Table IV can be set up. For all organic compounds of moderate polarity and not subject to H-bond formation, one obtains $V_p/V_m \simeq 0.6$. The same set of R_i's (Table I) produces V_m values that give a universal packing coefficient in molecular solids $C_K \simeq 0.7$[5]. We take the constance of these ratios as a hint that V_m does have a meaning in terms of long-range intermolecular interactions, although no quantitative interpretation is possible. For our purposes, this is an encouragement to consider V_m as a useful and meaningful molecular property.

For crystals, the following relationship was found to hold:[5]

$$E_t = 0.129V_m \tag{4}$$

where E_t (a computed quantity) is a sort of "theoretical" packing energy that can be interpreted as the lattice energy that would result if the crystal were a purely van der Waals one. If the computed E_t is smaller than compatible with the above equation, crystal forces other than van der Waals must be present (hydrogen bonds, ionic forces). E_t is always a lower-limit estimate (although often a close one) of the true sublimation energy of the crystal.

Application to Structured Media: Procedures

By "structured medium" is meant in the following, a system which presents a time-invariant alternance of empty and filled space; by empty and filled space is meant the space outside or inside the atomic spheres, respectively. Let us consider an envelope volume (V_{env}) as a parallelepiped defined by arbitrary boundaries within the medium: for our purposes it will be necessary to calculate the volume of any portion of empty or filled space within V_{env}. The use of eq 1 as such may not be convenient, since it gives an estimate of the global fraction of occupied space within V_{env}, not allowing distinction among different niches. Therefore, V_{env} is subdivided into smaller fractions, which will be called elementary volumes ($V_{el,i}$), tipically 0.2–0.5 Å^3. An analogue of eq 1 is then used within each $V_{el,i}$, giving D_i, the fraction of occupied space in the ith elementary volume:

$$D_i = (N_{occ}/N)_i \tag{5}$$

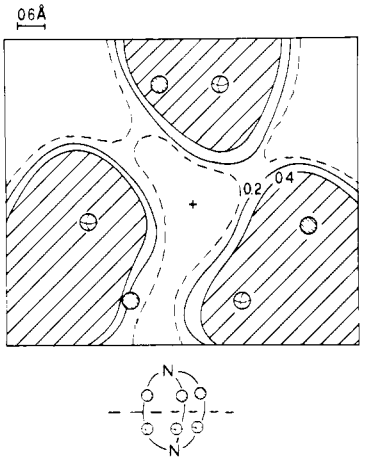

Figure 1. A section of the D_i map for the Na^+ cryptate complex (cation not included) in the plane shown by the dashed line in the molecular sketch below. Circles mark oxygen positions, the cross shows the position of the cation. The dashed curves enclose regions with $D_i < 0.10$. Dashed areas have $D_i > 0.4$.

Table V. Structural Data and Cavity Volumes for Cryptate Complexes of Alkali Metal Ions. Distances in Å, Volumes in Å^3

complex	Me$^+$-N distance, exptl[a]	Me$^+$-N distance, theor[b]	V_{hole}	V_{ion}[c]	$V_{hole,Me^+} - V_{hole,cryptand}$
cryptand			15.2		
Na^+	2.75	2.52	21.7	3.59	6.5
K^+	2.874	2.88	26.8	9.85	11.6
Rb^+	3.002	3.03	28.8	13.6	13.6
Cs^+	3.034	3.23	28.9	20.2	13.7

[a] From ref 16. [b] Sum of ionic radius and nitrogen van der Waals radius, see ref 16. [c] Based on ionic radii of Pauling: Pauling, L. "The Nature of the Chemical Bond"; Cornell University Press: Ithaca, 1960; p 514.

A three-dimensional map of D_i can be produced, spanning the whole extent of V_{env}. Holes and channels can be located by visual inspection of the map, and their volumes can be computed as

$$V_{hole} = \sum_{i,hole} (1 - D_i) V_{el,i} \qquad (6)$$

where the summation runs over all elementary volumes within the hole. Of course, the distribution of D_i's depends on the size of $V_{el,i}$; in principle, the shape and delimitation of cavities also do. Too large a mesh results in loss of resolution, while with a very small $V_{el,i}$ value cavities become interconnected. Fortunately, integral (summation) quantities like V_{hole} are less sensitive to the choice of the step, which can be considered as an adjustable parameter that can be optimized to focus the method for subtler quantitative applications. With our present choice for elementary volume size, cavities appear as reasonably well delimited and in tightly packed media, such as molecular crystals at low T, values of D_i smaller than 0.1 can seldom be found, whereas in more sparse media (like the cryptate cavities) holes of tens or hundreds of $D_i = 0$ can be found. The distinction between empty and filled space is thus a reasonably sharp one, since with our $V_{el,i}$ values the D_i drop at molecular boundaries is abrupt, and zones with $0.1 < D_i < 1.0$ usually give scarce contributions to hole volumes.

Cage Molecules: Cryptates

The simplest structured medium, by our definition, is a single cage molecule, such as the so-called cryptand **1**. **1** can coordinate

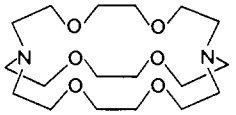

1

in its cavity a number of different ions; the molecular structures of **1** and its derivatives (cryptates) are known by X-ray diffraction.[16] The empty volume within the cage in **1** and its derivatives can thus be computed by drawing a D_i map through the molecule (not including the cation) and using eq 6. Figure 1 shows a sample portion of the map for the Na^+ cryptate; Table V summarizes the results. The volume of empty space, V_{hole}, was computed within the boundaries of the polyhedron defined by the positions of N and O atoms.

The map clearly shows the basic structural motif of these molecules as being made of three pillars encircling the ion, and hints at possible entrance or escape pathways for the ion, certainly favored by conformational flexibility in solution. The stability of cryptates, as judged by comparison of observed Me–O or Me–N distances with the corresponding sum of ionic and van der Waals radii,[16] reaches its peak for Rb^+; our data in Table V show that Rb^+ reaches almost perfect adaptation to the space made available by the "squashing" conformational change of the host molecule, using up the maximum extra volume that the host can provide. Cavity volume, as computed by our method, is thus a relevant quantity in the discussion of the stability of cryptates; presumably, it can be used to gauge the stability of many other solvation cages or transition-metal complexes, even if they have not been actually synthesized, once a reasonable structural hypothesis has been made.

Table VI. Properties of Perhydrotriphenylene Inclusion Compounds[b]

	PHTP (*n*-heptane)	PHTP (butadiene), **4**
space group	hexagonal, $P6_3/m$	monoclinic, $P2_1/m$
cell volume	858.4	849.2
V_m of PHTP	268	257
canal vol (per unit cell)	121	112
Z (PHTP)	2	2
Z (guest)	0.45	1
guest volume	58.0	68.6
C_K (PHTP alone)	0.624	0.605
C_K (PHTP + guest)	0.692	0.686
E_{pack}[a]	−49.2	−41.7

[a] Potential energy of the crystal; see ref 5 for details of the calculation of this quantity. [b] Crystal data from ref 17a and 19. Volumes in Å^3, energies in kcal/mol. Z is the number of molecules per unit cell, C_K is the Kitaigorodski packing coefficient. The E_{pack} is computed for the PHTP matrix alone.

Inclusion Compounds: Perhydrotriphenylene

Full-trans perhydrotriphenylene (PHTP) (**2**) provides a crys-

2

talline matrix consisting of a hexagonal structure of piles of molecules, among which vertical channels are formed;[17a] a wide variety of guest molecules can fit in these channels.[17b] Polymerization reactions can take place in PHTP matrices with a high degree of stereospecificity;[18] a sample case in which the crystal

(15) After completion of this work, we became aware that a method of molecular volume calculation similar to ours is mentioned in Meresse, A. Doctoral Thesis, Université de Bordeaux I, 1981, p 185.

(16) For the crystal structures and structural data of the complexes, see: Moras, D.; Weiss, R. *Acta Crystallogr., Sect. B* **1973**, *B29*, 396 and references therein. For the cryptand, see: Metz, B.; Moras, D.; Weiss, R. *J. Chem. Soc., Perkin Trans. 2* **1976**, 423. We thank Dr. G. Wypff, Université de Strasbourg, for bringing these compounds to our attention.

(17) (a) Colombo, A.; Allegra, G. *Atti Accad. Naz. Lincei* **1967**, *13*, 41. (b) Allegra, G.; Farina, M.; Immirzi, A.; Colombo, A.; Rossi, U.; Broggi, R.; Natta, G. *J. Chem. Soc. B* **1967**, 1020. Allegra, G.; Farina, M.; Colombo, A.; Casagrande-Tettamanti, G.; Rossi, U.; Natta, G. *Ibid.* **1967**, 1028.

(18) See, for a review: Farina, M. *Makromol. Chem., Suppl.* **1981**, *4*, 21.

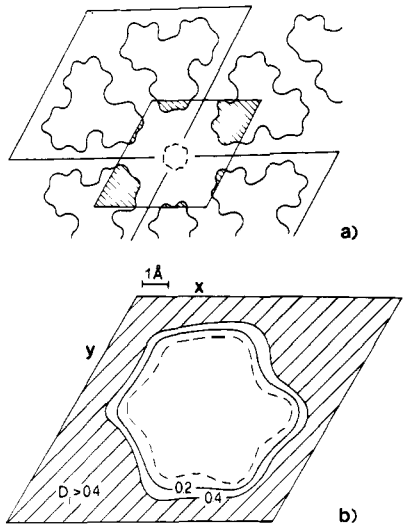

Figure 2. (a) The structural motif of the hexagonal PHTP crystal (after ref 17). Heavy solid lines are cell boundaries; the zone shown in (b) is delimited by lighter lines. (b) D_i map for PHTP in the channel zone. The dashed curves enclose the channel region, with $D_i < 0.10$.

Table VII. Percent Channel Occupancy Factors, C_C, for Inclusion Compounds in the Hexagonal Structure of PHTP[d]

guest	V_{guest}	Z_{guest}[a]	V_{occ}	C_C
n-pentane	95.0	0.57	54	45
n-heptane	128	0.45	58	48
n-tetradecane	246	0.25	62	51
n-C_{22}	380	0.16	61	50
benzene	85.4	0.76	65	54
toluene	102	0.61	62	52
bromoform[b]	84.0	0.64	54	45
chloroform[b]	69.1	1.00	69	57
cyclohexane	99.2	0.78	77	64
dioxane[b]	82.4	0.83	68	56
isooctane[b]	147	0.55	81	67
polymer 4	62.0	1.00	62	51
propyl ether[b]	119	0.49	58	48
butadiene[c]	68.6	1.00	69	62

[a] From ref 17. [b] V_{guest} computed by Bondi's volume increment table, ref 9. [c] Monoclinic PHTP crystal structure. [d] $V_{occ} = V_{guest}Z_{guest}$, and $C_C = 100(V_{occ}/V_C\lambda)$, where V_C is the canal volume in Table VII. All volumes in Å^3.

structures of reactants and products are known by X-ray analysis[19] is the reaction:

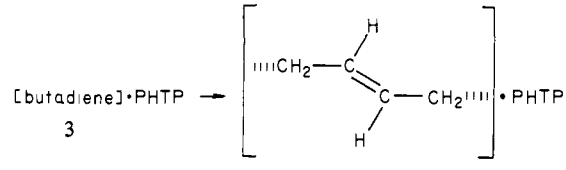

3 has a monoclinic crystal structure, while in **4** PHTP takes up the above-mentioned[17a] hexagonal structure. Figure 2a shows the basic motif of hexagonal PHTP, while Figure 2b shows a section of the corresponding D_i map in the region of the channel. Only the PHTP molecules have been included, and the free volume per unit cell (V_{canal}) has been computed. Table VI collects observed and calculated quantities for the two PHTP structures mentioned so far.

The number of guest molecules per cell can be obtained from X-ray analysis of the crystals;[17b] reducing all available data[17,19] to the standard hexagonal cell of PHTP, with two PHTP molecules, and calculating the guest molecular volume (not necessarily the volume of an integer number of molecules), one obtains the data in Table VII.

(19) Colombo, A.; Allegra, G. *Macromolecules* **1971**, *4*, 579.

The map shown in Figure 2b illustrates the potentiality of the volume analysis: by drawing such maps in a systematic way, the shape of the cavity can be accurately determined. Many structures could be tested, by introducing guest atoms in the calculation in different positions, and checking for the resulting free space, to find the best close-contact structure. From Table VI it can be seen that the hexagonal structure for PHTP provides a slightly larger empty space, but is more tightly packed than the monoclinic one, as judged from the values of C_K and of the packing energy. The monoclinic structure is more efficient in lodging its butadiene guest that occupies 68.6 Å^3 per cell, but remarkably enough both structures reach the same overall host + guest overall packing coefficient $C_K \simeq 0.7$, fully compatible with the close-packing principle.

The data in Table VII can be interpreted as follows. Linear chain compounds have a constant channel occupancy factor $C_c \simeq 50\%$, which leads to the equation

$$Z_{guest} \simeq 60/V_{guest} \quad (7)$$

for the number of guest molecules per cell. This allows a prediction of the stoichiometry of the inclusion compounds; such a regular behavior undoubtedly originates from the fact[20] that the packing energy of *n*-alkanes in their own crystals is made up of independent and additive contributions from each methylene group. Higher C_C values pertain to cyclic or globular molecules such as benzene or chloroform; peak C_C values are attained by cyclohexane and the highly branched isooctane molecule. It can be stated that if $C_C > 50\%$ the structure of the guest molecule must be branched or cyclic. Since V_{guest} does not vary very much among different isomers, this information can be useful in an independent assessment of the amount of branching in the products of inclusion reactions.

Applications to Solid-State Reactivity

A general theory of organic reactions in the solid state is not yet available. Ideally, a sound relationship between crystal structure and reactivity would be required. We wish to exploit here the idea that a prerequisite for crystal reactivity is the availability of free space around the reaction site: reactive crystals obey the close-packing principle on the whole, but local breakdowns of this principle (holes or channels in the crystal structure) can assist the reaction in its former stages. This idea pays a tribute to the reaction cavity concept and the topochemical postulate,[21] but the volume analysis made possibly by D_i maps is a step toward quantification of both. It should be noted that the Fourier synthesis maps of usual X-ray crystal structure analysis do not lend themselves to the same purpose, being largely influenced by data treatment and truncation, thus not allowing a sharp definition of filled and empty space.

Maps of D_i have been computed for some cases of well-known reactive crystals, in order to spot packing irregularities. The first case we have analyzed is that of the reaction of azobis(isobutyronitrile), AIBN:[22]

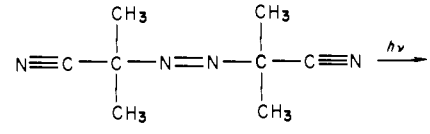

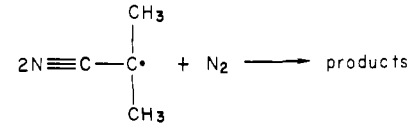

(20) Filippini, G.; Gavezzotti, A.; Simonetta, M.; Mason, R. *Nouv. J. Chim.* **1981**, *5*, 211.

(21) See ref 10 and references therein. The volume analysis method was presented in preliminary form at the VI International Conference on the Chemistry of the Organic Solid State, Freiburg, 1982; see: Gavezzotti, A. *Mol. Cryst. Liq. Cryst.* in press.

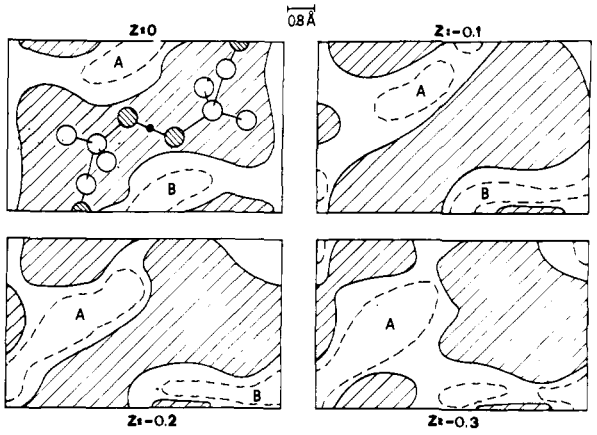

Figure 3. Sections (perpendicular to the z axis) of the D_i map for the AIBN crystal. x (horizontal) and y (vertical) for each section go from $-1/2$ to $+1/2$. Note that γ (=79.2°) appears as 90°, so the maps are slightly distorted. Dashed curves enclose regions with $D_i < 0.10$; the volume of cavity A is 6.8 Å^3.

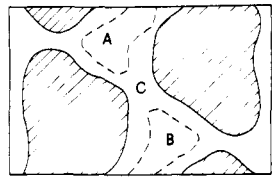

Figure 4. Same as section $z = 0$, Figure 3, but diazo N atoms have been omitted from the D_i calculation.

The solid-state products of the reaction are mainly isobutyronitrile and methacrylonitrile, indicating that no radical encounter leading to dimers takes place. The dipoles of the nitrile groups apparently hold the radicals in place in the crystal, as they did with the original AIBN molecule.

The D_i map for AIBN is shown in Figure 3. It is indicative of the packing mode of this compound, which consists basically of a parallel arrangement of molecules, with vast (7 Å^3) pockets of intermolecular free space (labeled A and B in the figure; note that A and B are symmetry related). We propose that reactivity in AIBN crystals is greatly favored, on a kinetic ground, by the breakdown of the close-packing principle represented by the cavities in proximity of the –N=N– group. These cavities provide space for the incipient N_2 molecule, and help relax the otherwise prohibitive internal stress that results from its formation. A D_i map drawn without the contribution of the central N atoms (Figure 4) shows that (as expected) the resulting cavity (C) communicates with the preexisting A and B channels, and that the two radicals are separated by a wide gap, a fact that has consequences on their final fate.

The second case examined is that of the radical reaction of acetyl benzoyl peroxide, ABP:[23]

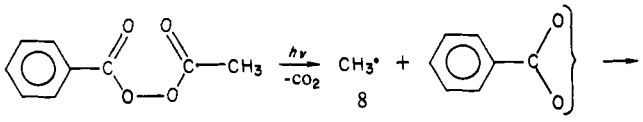

7 8 9

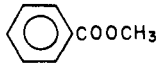

10

This reaction is an ideal test case for our methods, since large displacements of the reactive fragments are required and products form by collapse of fragments from one precursor molecule in their cage. Moreover, the reaction is selective in that the methyl radical, **8**, becomes attached preferentially to the peroxy oxygen of the benzoyloxy radical, **9**.

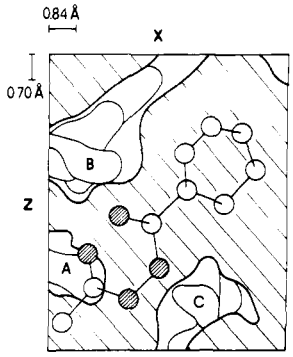

Figure 5. D_i map for the ABP crystal, obtained by superimposition of sections perpendicular to the y axis. Cavities A, B, and C are delimited by the superimposition of curves enclosing zones with $D_i < 0.10$. x (horizontal) goes from $-1/2$ to $+1/2$, z (vertical) from –0.65 to –0.10 (all values in fractional units). Note that $\beta = 97.2°$ and the scales on x and z differ, so that the map is slightly distorted.

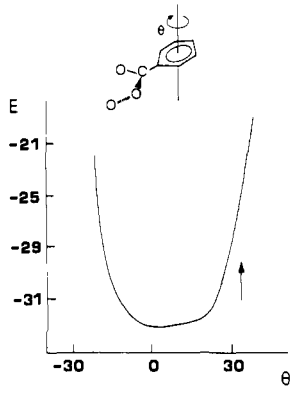

Figure 6. Packing potential energy (E) curve as a function of θ, the angle of in-plane rotation of the benzoyloxy radical (as shown above). 0° is the position before reaction, and the vertical arrow marks the proposed (see ref 23b) position after radicalization. The units are kcal/mol and degrees.

Two possible mechanisms have been envisaged: (a) **9** does not move, CO_2 is detached and moves in between the methyl radical and the carbonyl oxygen of **9**, ester is formed to the peroxy oxygen of **9**;[23a] (b) **8** is less mobile, and the stress induced by incipient CO_2 pushes **9** to rotate in its molecular plane, thus bringing the peroxy oxygen in front of radical **8** for reaction.[23b] Our D_i map (Figure 5) shows three cavities in the surroundings of the reaction site, labeled A, B, and C. If (a) is true, then the CO_2 molecule moves upwards into cavity A. In view of the vast amount of space around the COO group of **9**, it is difficult to believe that the benzoyloxy radical would be motionless during the reactions: the observed[23b] 30° rotation would shift the COO group so as to fit nicely into cavity B (although it may not be evident at first sight, cavity C is not correctly positioned to receive the COO group after rotation in the opposite sense). A simple energetic counterpart of this volume argument is shown in Figure 6: the packing potential energy profile for rotation of **9** in its molecular plane is much flatter in the direction of the observed 30° rotation, which, even if the crystal environment is unaltered, requires as little as 6 kcal/mol activation.

Figure 6 is the illustration of the concept that free space in crystals encourages "soft" (that is, low activation energy) displacements of properly oriented molecules toward holes or cavities in the crystal structure: in an ordered crystal, such librations can in principle be observed by phonon spectroscopy, and the concepts of phonon-assisted reactions has been introduced.[24] A flat po-

(22) Jaffe, A. B.; Malament, D. S.; Slisz, E. P.; McBride, J. M. *J. Am. Chem. Soc.* **1972**, *94*, 8515 and references therein. Our calculations were based on the $P\bar{1}$ modification of AIBN.

(23) (a) Karch, N. J.; Koh, E. T.; Whitsel, B. L.; McBride, J. M. *J. Am. Chem. Soc.* **1975**, *97*, 6729. (b) McBride, J. M.; Merrill, R. A. *Ibid.* **1980**, *102*, 1723. McBride, J. M., personal communication.

(24) Dwarakanath, K.; Prasad, P. N. *J. Am. Chem. Soc.* **1980**, *102*, 4254.

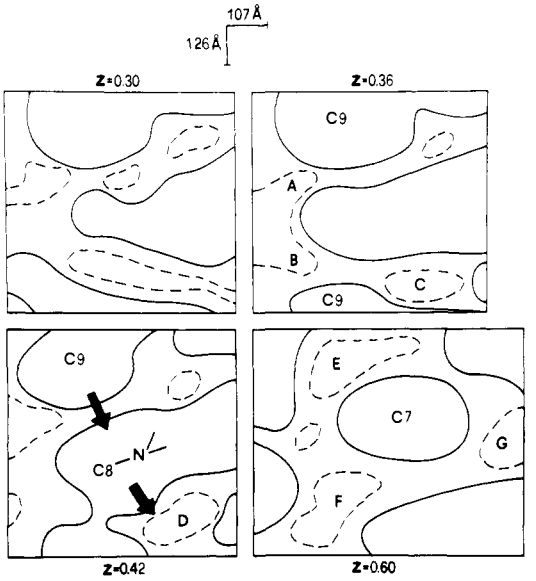

Figure 7. Sections (perpendicular to z) of the D_i map for the DMABS crystal. The dashed curves enclose zones with $D_i < 0.10$ and full lines enclose zones with $D_i > 0.7$. Arrows mark displacements of the reacting groups in the crystal; note that as C9 is pushed forwards for reaction, the volume of cavity D is increased, thus favoring cooperation. x (horizontal) goes from −0.10 to +0.56 and y (vertical) from 0 to +0.78 for each section (all values in fractional units). For $z = 0.6$, x runs to +0.63.

tential energy profile has been calculated[25] for the pyramidal bending of the dimethylamino group in the reaction of (*p*-(dimethylamino)benzene)sulfonate (DMABS), **11**, in the solid state:[26]

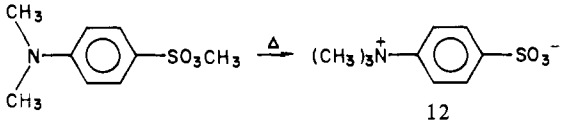

11 12

This case will be our third example of packing analysis. The volume analysis in the strategic regions of the DMABS crystal (see the D_i maps in Figure 7) clearly reveals that the three methyl groups involved in the reaction are surrounded by large zones of free space. The sulfonium ester methyl group (labeled C9) is encircled by cavities A, B, and C, so that it can be classified as a highly mobile group. More specifically, the N and C8 atoms have a pocket of free space (D in Figure 7) exactly in the correct position to allow pyramidalization at the would-be tetrahedral ammonium center after attack by C9; and finally C7, the second amino methyl group, has plenty of extra space to move in (see zones E, F, and G in Figure 7). Actually, the structural backbone of the DMABS crystal is formed by regular head-to-tail stacks of molecules held together presumably by electrostatic forces between N and SO_3 centers; the position of terminal methyl groups being in a sense a by-product of this basic arrangement, these groups may be subject to less stringent close-packing requirements, and may be relatively loosely packed. The overall packing efficiency in the DMABS crystal is quite normal ($C_K = 0.69$), but local breakdowns of close packing facilitate the reaction by providing empty space where needed. This information could probably be recast in spectroscopic language by analyzing the components of the related lattice vibrations.

(25) Gavezzotti, A.; Simonetta, M. *Nouv. J. Chim.* **1977**, *2*, 69.
(26) Sukenik, C. N.; Bonapace, J. A. P.; Mandel, N. S.; Lau, P.; Wood, G.; Bergman, R. G. *J. Am. Chem. Soc.* **1977**, *99*, 851.

Final Remarks

Molecular volume can be rapidly and accurately computed by using molecular geometry and atomic radii. It is a useful molecular property, and its numerical value is not too sensitive to small variations in the input information. Less immediate is its interpretation in terms of quantum chemistry, but this interpretation is unnecessary for the present purposes.

When accepted on such basis, the concept of molecular volume introduces the concept of volume analysis in structured media, in the very simple terms of empty and filled space. This analysis is the intermolecular analogue of steric hindrance effects, as usually discussed in all theories of molecular transformations. When applied to fully or partially ordered media, our volume analysis allows a clear identification and a partial quantification of steric effects, which in such media appear as strategically located holes of empty space.

We have presented some applications of the method, but many more can be envisaged (in studies of enzyme–substrate compatibility; in the chemistry of solvation, cage compounds, and transition-metal complexes; in catalysis by inclusion in zeolites; in studies of solid–gas reactions in which channels in the crystal structure allow selective diffusion of the gas in the solid). Our main emphasis here is in applications to solid-state reactions which require mobility—and hence free space—in their initial stages, when the crystal structure is not yet distorted by product formation.[23] Maps like the one shown in Figure 5 may not be stringent proof of mechanism, but they certainly point out at once the steric terms on which mechanism has to be discussed. Besides, their simple and readily obtainable information provides a good starting point in the interpretation of spectroscopic experiments on the displacement of reaction fragments.

Widespread use of the method is encouraged, and the computer programs are available for distribution.

Registry No. 1, 23978-09-8; **1**·Na^+, 32611-94-2; **1**·K^+, 23978-09-8; **1**·Rb^+, 32611-96-4; **1**·Cs^+, 32614-32-7; **2**, 16069-13-9; **2**·*n*-pentane inclusion compound, 86287-14-1; **2**·*n*-heptane inclusion compound, 64474-25-5; **2**·*n*-tetradecane inclusion compound, 86287-15-2; **2**·*n*-C_{22} inclusion compound, 86287-16-3; **2**·benzene inclusion compound, 86287-17-4; **2**·toluene inclusion compound, 86287-18-5; **2**·bromoform inclusion compound, 86287-19-6; **2**·chloroform inclusion compound, 58904-68-0; **2**·cyclohexane inclusion compound, 86287-20-9; **2**·dioxane inclusion compound, 86287-21-0; **2**·isooctane inclusion compound, 86287-22-1; **2**·propyl ether inclusion compound, 86287-23-2; **3**, 86287-24-3; **4**, 86287-81-2; **5**, 78-67-1; **7**, 644-31-5; **11**, 57270-54-9.